Automatic Material Classification of Targets from GPR Data using Artificial Neural Networks

Nairit Barkataki
Dept. of Instrumentation & USIC
Gauhati University
Guwahati, India

Ankur Jyoti Kalita
Dept. of Instrumentation & USIC
Gauhati University
Guwahati, India

Utpal Sarma
Dept. of Instrumentation & USIC
Gauhati University
Guwahati, India

2022 IEEE Silchar Subsection Conference (SILCON) | 978-1-6654-7100-8/22/$31.00 ©2022 IEEE | DOI: 10.1109/SILCON55242.2022.10028944

***Abstract*—Ground penetrating radar (GPR) is a preferred non-destructive method to study and identify buried objects in the field of geology, civil engineering, archaeology, military, etc. Landmines are now largely composed of plastic and other non-metallic materials, while archaeologists must deal with buried artefacts such as ceramics, pillars, and walls built of a range of materials. As a result, understanding the material properties of buried artefacts is critical. This study presents an ANN model for automatic classification of buried objects from GPR A-Scan data. The proposed ANN model is trained and validated using a synthetic dataset generated using gprMax. The model performs well in classifying three different object classes of aluminium, iron and limestone, while achieving an overall accuracy of 95%.**

***Index Terms*—deep learning, artificial neural network, classification, object material, ground penetrating radar**

I. Introduction

Understanding and studying the subsurface of the earth is crucial in geology, civil engineering, archaeology, military, and other fields. There is a growing need for non-invasive techniques to explore and retrieve information about the underground, whether to determine soil properties or to locate and characterise unknown objects. Ground penetrating radar (GPR) is a popular method for subsurface mapping and the detection of underground objects like electrical lines [1], land mines [2], pipes [3], road inspection [4], etc. Nowadays, landmines are mostly made out of plastic and other non-metallic materials. Moreover, archaeologists have to deal with buried artefacts like pottery, pillars, walls etc. which are made of a variety of materials like limestone, iron, wood etc. Hence, knowledge of the material properties of buried objects is of vital importance to investigators across all fields.

GPR has been frequently used to locate underground structures in a non-destructive manner. Other non-destructive tools are also used to map the subsurface. Al-Qubaa et al. [5] constructed a Giant Magneto-Resistive (GMR) sensor array to capture scattered EM signal reflected by different metallic objects. They extracted features like shape, properties and transient response analysis to identify handguns. Saripan et al. proposed a method to identify the types of materials buried in sand by collecting the scattered components of a gamma-ray radiation [6]. Several feature points were then taken from the frequency domain of the acquired signals for ANN classification of material types. Setyabudi et al. proposed an ANN model to classify metallic and non metallic object based on the seismic vibrations propagating in the ground measured by an accelerometer [7]. The above-mentioned techniques suffered from limitations like slow data collection, limited depth, low resolution etc.

Ni et al. enriched raw GPR data using the Discrete Wavelet Transform (DWT) [3]. This resulted in better profile images and they were able to classify between pipes made of plastics and metals. A new feature extraction method was proposed by Lu et al. using DWT and Fractional Fourier Transform (FRFT) [8]. The extracted features were fed to Support Vector Machine (SVM) classifier to automatically detect subsurface items and materials from GPR A-Scans. Park et al. used a phase analysis technique on GPR data to isolate subsurface cavities and potential sinkholes from other underground objects. Background filtration of 3D GPR data was performed to highlight the electromagnetic waves reflected only from underground objects to make underground objects more visible [9].

Machine learning based interpretation of GPR data is gaining popularity nowadays. Machine learning and deep learning based techniques have been applied to GPR data for various kind of tasks like object detection [10] and size estimation [11], detection of landmines [12], hyperbolic pattern recognition [13], soil moisture estimation [14], soil type classification [15], etc. Núñez et al. proposed an automated detection system for subsurface explosive artefacts using machine learning algorithms [16]. Safatly et al. used Convolutional Neural Network (CNN) to classify buried objects including mines or other items based on the metal detector signature [17]. The accuracy of their proposed model was almost 90%. Pasolli et al. utilised SVM to classify buried objects such as air, metal, and limestone from GPR images and achieved an accuracy of 84% [18]. Numerous research have shown that applying deep learning algorithms significantly improves performance for classification issues of GPR data. Using a two-dimensional (2D) grid image made up of a number of GPR B-scan and C-scan images, Kim et al. employed deep CNN to classify between subsoils, pipes, cavities, and manholes [19]. Ali et al. extracted important signatures from hyperbolic features in GPR B-Scans using statistical techniques [20]. They were able to design neural network based binary classifier to classify between metals and non-metals. CNN based classifier was

used by Elsaadouny et al. to discriminate real landmines from other mine-shaped objects in GPR images [21].

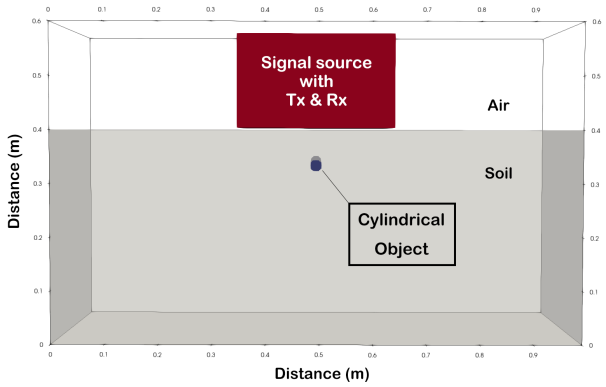

Fig. 1. Simulated model

Although numerous techniques have been employed to identify various kinds of buried objects, there is ample scope of research to classify different kinds of buried materials using GPR data. This paper mainly focuses on

1) The creation of a synthetic GPR database containing buried objects of different materials.
2) The development of an ANN model to classify objects based on their materials using GPR data.

II. GPR Data

GprMax [22], a open-source GPR simulator, is used to create the dataset for this study. The dimensions of the model are 990 $mm \times 400\ mm \times 600\ mm$ ($X \times Y \times Z$). The top 200 mm of the simulated model is a layer of air, while the bottom 400 mm is a layer of soil, as shown in the Figure 1.

Cylindrical objects of three different materials are placed between 150 mm and 360 mm underneath the soil's surface. The objects are made of aluminium, iron, and limestone having relative permittivity and conductivity given in Table I.

The simulation parameters for the model are given in Table II. Simulations are accelerated using NVIDIA GPU RTX 3090 [23]. The A-Scans of buried objects of different materials is shown in Figure 2. The relative permittivity (ε_r) of the soil used for the simulation is 10 and the conductivity (σ) is 0.002 S/m. A time window of 14 ns is used in this study.

TABLE I
RELATIVE PERMITTIVITY AND CONDUCTIVITY OF THE BURIED CYLINDRICAL MATERIALS

Object Type	**Relative Permittivity** ε_r	**Conductivity** σ **(S/m)**
Aluminium	10.8	3.5×10^{7}
Iron	1.45	9.98×10^{6}
Limestone	5.8	9×10^{-3}

TABLE II
GPRMAX SIMULATION PARAMETERS

Sl. No.	**Simulation Parameters**	**Values**
1	Excitation waveform	Gaussian
2	Antenna frequency	400 MHz
3	Time window	14 ns
4	Spatial resolution	2 mm
5	Maximum radius of the cylindrical object	30 mm
6	Minimum radius of the cylindrical object	10 mm

A. Data Preprocessing

A total of 9300 A-Scans are generated. The dataset is built by concatenating all the A-Scans forming an array of dimensions 9300×3631, together with their corresponding labels (aluminium, iron, limestone).

III. Methodology

ANN is used to classify the buried objects based on their material types. 7400 A-Scan samples (80%) out of the 9300 A-Scans are utilised for training, while 1860 samples (20%) are used to validate the model's performance. The output of each neuron is defined by an activation function, and the error is monitored by a loss function. The goal is to reduce the loss. The data is normalised before training.

A. The Proposed Model

Several training runs show that the ANN model containing six hidden layers is the most accurate and reliable. Its architecture is shown in Figure 3.

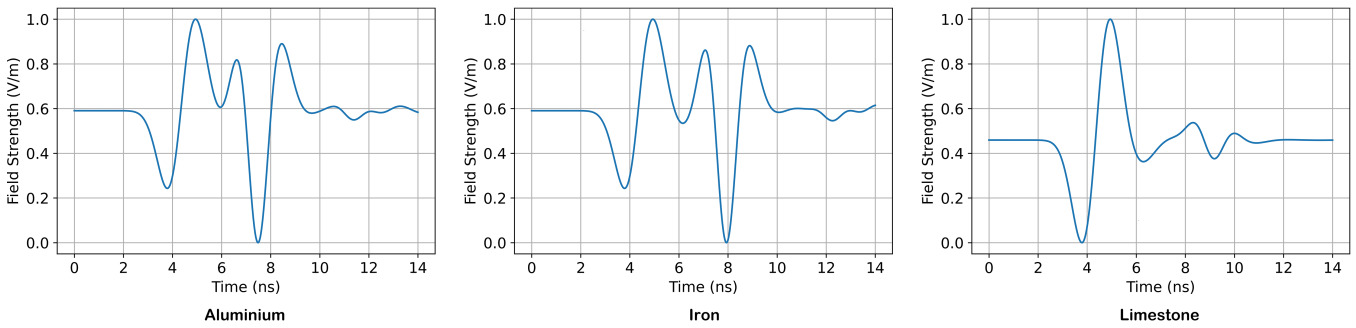

Fig. 2. A-Scans of three objects of different material buried underneath the soil

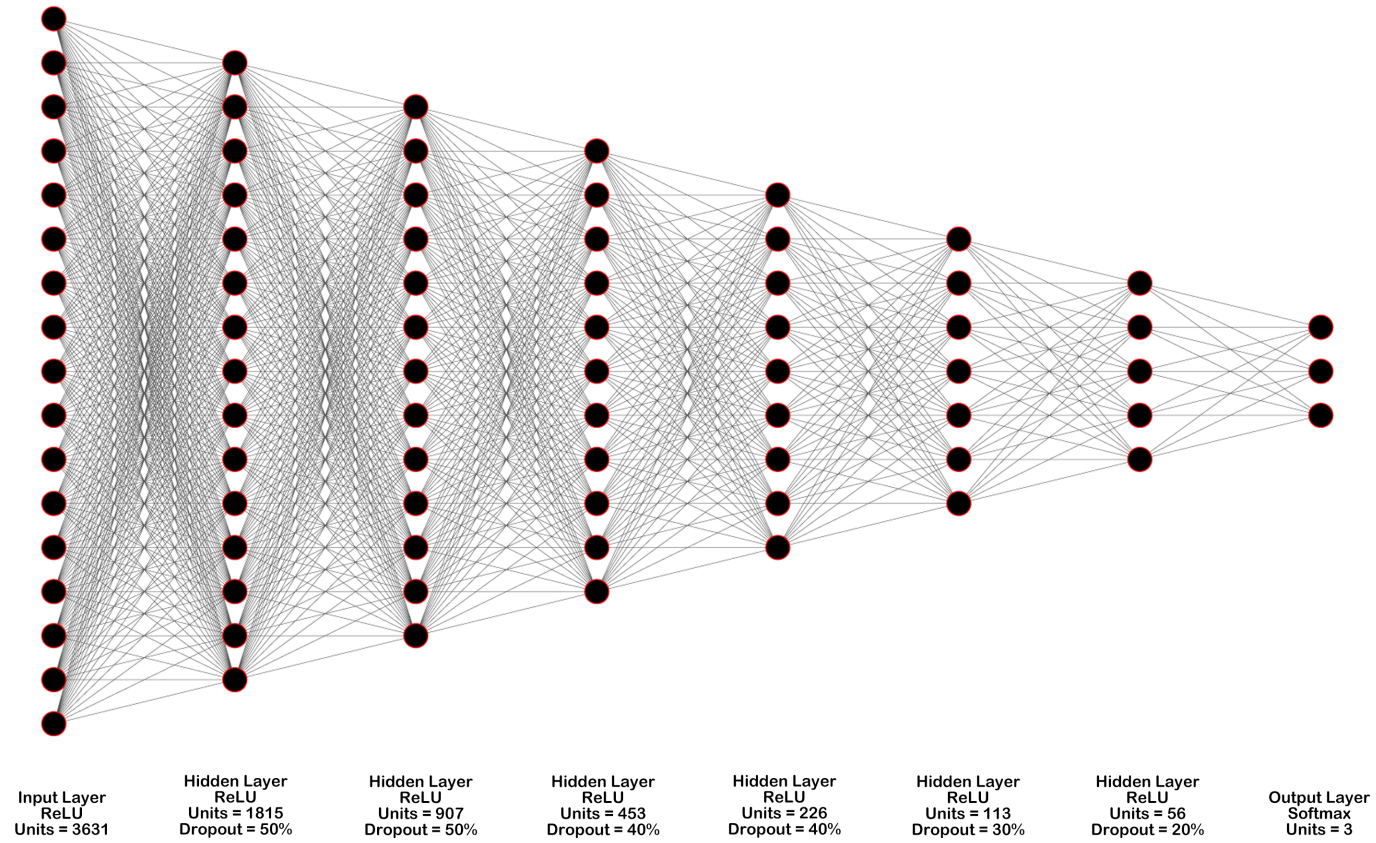

Fig. 3. Proposed architecture for ANN

Initially, 3631 neurons were used in the neural network's input layer followed by a series of hidden layers, each containing half as many neurons as the layer before it. There are 1815, 907, 453, 226, 113, and 56 neurons in each of these six hidden layers, respectively. ReLU (Rectified Linear Unit) activation function is used in all the layers. ReLU is a non-linear function which sets all negative input values to 0. All other values are kept constant. Mathematically, it is expressed as given in equation 1.

$$f(n) = max(0, n) \quad (1)$$

where n is neuron input.

For the classification of the buried objects, three neurons are employed in the output layer with softmax activation function. Categorical cross-entropy is utilised as the loss function in the model.

Adadelta algorithm is used for optimising the model, which is a more robust extension of Adagrad that adapts learning rates based on a moving window of gradient updates, instead of accumulating all past gradients. This way, Adadelta continues learning even when many updates have been done. The learning rate of Adadelta is taken to be the default one which is 0.001 as it benefits from higher initial learning rate compared to other optimizers [24].

Dropout layers are employed in the proposed model to prevent overfitting of the model by randomly setting input neurons to zero with a frequency of rate at each step during training time. The second and third layers of the proposed model employ a dropout rate of 50%, the fourth and fifth layer a dropout rate of 40%, the sixth layer a dropout rate of 30%, and the seventh layer a dropout rate of 20%.

IV. Results

An overall accuracy of 95% is obtained after numerous training and validation runs. Different metrics, including precision, recall, and F1-score are calculated for each of the three material classes in order to evaluate the model's performance as shown in Table III. The model's confusion matrix is depicted in Figure 4 with the actual class labels on the y-axis and the predicted class labels on the x-axis.

TABLE III
Classification Report of the ANN Model

Object Shape	Precision	Recall	F1-score	Accuracy
Aluminium	0.92	0.93	0.93	
Iron	0.93	0.90	0.91	95%
Limestone	1.00	1.00	1.00	

TABLE IV
COMPARISON WITH PAST STUDIES

Sl. No.	Authors	Technique used	Classes	Accuracy
1	Setyabudi et al. [7] (2019)	ANN applied on Seismic vibrations	2 metallic and non metal	77%
2	Lu et al. [8] (2014)	DWT-FRFT feature-based SVM on GPR data	3 PEC, stone, PVC	92%
3	Saripan et al. [6] (2013)	ANN applied on scattered components of a gamma-ray radiation	3 wood, stone, stainless steel	48%- 95%
4	Pasolli et al. [18] (2009)	SVM applied on GPR images	3 air, metal (PEC), limestone	84%
5	**Present work**	ANN applied on GPR data	3 aluminium, iron, limestone	95%

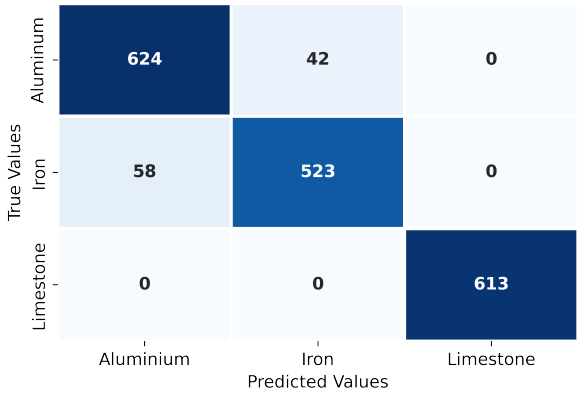

Fig. 4. Confusion matrix of the ANN Model

Precision (P) refers to a classifier's ability to measure how many of the positive predictions made are correct. The accuracy of categorising an aluminium object in Figure 4 can be computed using the formula in equation 2. Only 624 of the 682 aluminium materials are categorised as such.

$$Precision = \frac{624}{682} = 0.92 \tag{2}$$

The classifier's capacity to tell what proportion of all positive cases the model accurately predicts is measured by Recall (R). For each class in Figure 4, it is the ratio of True Positive and the sum of True Positive and False Negative. Out of the total 666 predictions for aluminium object, 624 were accurate, while 42 were false negatives. Recall for aluminium object can therefore be estimated as per equation 3.

$$Recall = \frac{624}{666} = 0.93 \tag{3}$$

F1-score is a metric used to assess how well a model performs in terms of classification and can be interpreted as a weighted average of the precision and recall. It ranges from 0 to 1, with 1 being a perfect score, meaning that the model accurately predicted each observation. The F1-score can be determined using the classifier's precision and recall for the aluminium object as indicated in equation 4.

$$F1 - Score = 2 \times \frac{P \times R}{P + R} = 0.93 \tag{4}$$

V. CONCLUSION

An ANN model for automatic classification of buried object based on their material types was presented in this study. From the classification report in Table III and confusion matrix in Figure 4, it is seen that the proposed model is able to classify different materials with a high degree of accuracy. The model is able to classify metallic (aluminium / iron) and non-metallic objects (limestone) with 100% accuracy. The accuracy decreases when trying to classify between objects made of aluminium and iron. Table IV provides a comparison with previously published literature work. The previously reported studies dealt with binary classification, used less data for testing and validation, or suffered from slow data collection. In other cases, their reported classification accuracy was less than the present work. The present work, which uses GPR, will speed up the collection of data and allow for real-time results for material classification. This can be very useful in fields like landmine detection, archaeology, civil engineering etc. where knowledge of materials is crucial for taking on-field decisions.

Limitations

The proposed model is trained and tested on synthetic data and is yet to be tested with real data. Objects of only three different materials were considered while generating the GPR data. Moreover, all the objects in this study were of cylindrical shapes. The authors plan to add more shapes based on different materials to validate the model with experimental data.

VI. ACKNOWLEDGEMENT

The author would like to thank Mr. Anirban Bhattacharjee and Ms. Sharmistha Mazumdar for their help during the generation of the dataset. The authors would like to point out that without Google Colaboratory, training and validating the model would have been a time consuming task.

REFERENCES

[1] N. Šarlah, T. Podobnikar, T. Ambrožič, and B. Mušič, "Application of kinematic gpr-tps model with high 3d georeference accuracy for underground utility infrastructure mapping: A case study from urban sites in celje, slovenia," *Remote Sensing*, vol. 12, no. 8, p. 1228, 2020.

[2] K. Ishitsuka, S. Iso, K. Onishi, and T. Matsuoka, "Object detection in ground-penetrating radar images using a deep convolutional neural network and image set preparation by migration," *International Journal of Geophysics*, vol. 2018, 2018.

[3] S.-H. Ni, Y.-H. Huang, K.-F. Lo, and D.-C. Lin, "Buried pipe detection by ground penetrating radar using the discrete wavelet transform," *Computers and Geotechnics*, vol. 37, no. 4, pp. 440–448, 2010.

[4] M. Rasol, J. C. Pais, V. Pérez-Gracia, M. Solla, F. M. Fernandes, S. Fontul, D. Ayala-Cabrera, F. Schmidt, and H. Assadollahi, "Gpr monitoring for road transport infrastructure: A systematic review and machine learning insights," *Construction and Building Materials*, vol. 324, p. 126686, 2022.

[5] A. R. Al-Qubaa, A. Al-Shiha, and G. Y. Tian, "Threat target classification using ann and svm based on a new sensor array system," *Progress In Electromagnetics Research B*, vol. 61, pp. 69–85, 2014.

[6] M. I. Saripan, W. H. M. Saad, S. Hashim, A. T. A. Rahman, K. Wells, and D. A. Bradley, "Analysis of photon scattering trends for material classification using artificial neural network models," *IEEE Transactions on Nuclear Science*, vol. 60, no. 2, pp. 515–519, 2013.

[7] M. R. Setyabudi and R. Mardiyanto, "Buried object detection based on acousto-seismic method using accelerometer and neural network," *ICASESS 2019*, p. 252, 2020.

[8] Q. Lu, J. Pu, and Z. Liu, "Feature extraction and automatic material classification of underground objects from ground penetrating radar data," *Journal of Electrical and Computer Engineering*, vol. 2014, 2014.

[9] B. Park, J. Kim, J. Lee, M.-S. Kang, and Y.-K. An, "Underground object classification for urban roads using instantaneous phase analysis of ground-penetrating radar (gpr) data," *Remote Sensing*, vol. 10, no. 9, p. 1417, 2018.

[10] H. Liu, C. Lin, J. Cui, L. Fan, X. Xie, and B. F. Spencer, "Detection and localization of rebar in concrete by deep learning using ground penetrating radar," *Automation in construction*, vol. 118, p. 103279, 2020.

[11] N. Barkataki, B. Tiru, and U. Sarma, "A cnn model for predicting size of buried objects from gpr b-scans," *Journal of Applied Geophysics*, vol. 200, p. 104620, 2022.

[12] S. Lameri, F. Lombardi, P. Bestagini, M. Lualdi, and S. Tubaro, "Landmine detection from gpr data using convolutional neural networks," in *2017 25th European Signal Processing Conference (EUSIPCO)*. IEEE, 2017, pp. 508–512.

[13] Q. Dou, L. Wei, D. R. Magee, and A. G. Cohn, "Real-time hyperbola recognition and fitting in gpr data," *IEEE Transactions on Geoscience and Remote Sensing*, vol. 55, no. 1, pp. 51–62, 2016.

[14] N. Barkataki, S. Mazumdar, B. Tiru, and U. Sarma, "Estimation of soil moisture from gpr data using artificial neural networks," in *2021 IEEE International Conference on Technology, Research, and Innovation for Betterment of Society (TRIBES)*. IEEE, 2021, pp. 1–5.

[15] N. Barkataki, S. Mazumdar, P. B. D. Singha, J. Kumari, B. Tiru, and U. Sarma, "Classification of soil types from GPR B scans using deep learning techniques," in *2021 6th IEEE International Conference on Recent Trends in Electronics, Information & Communication Technology (RTEICT 2021)*, August 2021, pp. 840–844.

[16] X. Núñez-Nieto, M. Solla, P. Gómez-Pérez, and H. Lorenzo, "Gpr signal characterization for automated landmine and uxo detection based on machine learning techniques," *Remote sensing*, vol. 6, no. 10, pp. 9729–9748, 2014.

[17] L. Safatly, M. Baydoun, M. Alipour, A. Al-Takach, K. Atab, M. Al-Husseini, A. El-Hajj, and H. Ghaziri, "Detection and classification of landmines using machine learning applied to metal detector data," *Journal of Experimental & Theoretical Artificial Intelligence*, vol. 33, no. 2, pp. 203–226, 2021.

[18] E. Pasolli, F. Melgani, and M. Donelli, "Automatic analysis of gpr images: A pattern-recognition approach," *IEEE Transactions on Geoscience and Remote Sensing*, vol. 47, no. 7, pp. 2206–2217, 2009.

[19] N. Kim, S. Kim, Y.-K. An, and J.-J. Lee, "A novel 3d gpr image arrangement for deep learning-based underground object classification," *International Journal of Pavement Engineering*, vol. 22, no. 6, pp. 740–751, 2021.

[20] H. Ali, A. A. Firdaus, M. S. Z. Azalan, S. Kanafiah, S. Salman, M. Ahmad, T. S. T. Amran, and M. S. M. Amin, "Classification of different materials for underground object using artificial neural network," in *IOP Conference Series: Materials Science and Engineering*, vol. 705, no. 1. IOP Publishing, 2019, p. 012013.

[21] M. Elsaadouny, J. Barowski, and I. Rolfes, "The subsurface objects classification using a convolutional neural network," in *2019 IEEE 10th Annual Information Technology, Electronics and Mobile Communication Conference (IEMCON)*. IEEE, 2019, pp. 0874–0877.

[22] C. Warren, A. Giannopoulos, and I. Giannakis, "gprmax: Open source software to simulate electromagnetic wave propagation for ground penetrating radar," *Computer Physics Communications*, vol. 209, pp. 163–170, 2016.

[23] C. Warren, A. Giannopoulos, A. Gray, I. Giannakis, A. Patterson, L. Wetter, and A. Hamrah, "A cuda-based gpu engine for gprmax: Open source fdtd electromagnetic simulation software," *Computer Physics Communications*, vol. 237, pp. 208–218, 2019.

[24] F. Chollet *et al.*, "Keras," `https://keras.io`, 2015.